JOURNAL OF SPACECRAFT AND ROCKETS
Vol. 35, No. 3, May–June 1998

Stiffness Design of Deployable Satellite Antennas in Deployed Configuration

Masayoshi Misawa*
Nippon Telegraph and Telephone Corporation, Kanagawa 238-03, Japan
and
Yoshiaki Ohkami†
Tokyo Institute of Technology, Tokyo 152, Japan

A new design method is described that ensures the first frequency of deployable satellite antennas in the deployed configuration. Deployable satellite antennas are modeled as a coupled system; the reflector (an elastic body) is supported by an antenna deployment mechanism (a coil spring). The displacement of the reflector in the system is expressed as the sum of the elastic displacement and the rigid-body displacement due to spring rotation. The system vibration equation is obtained by substituting kinetic and potential energies into Lagrange's equation. An eigenvalue problem is solved for the coupled system to obtain frequency relationships. A procedure is presented to establish stiffness requirements of the antenna deployment mechanism so that the deployable antennas can meet the frequency requirements. To confirm the proposed design method, calculations were made on the deployable antenna for the Japanese Experimental Test Satellite VI. The actual frequency of the deployable antenna was measured in orbit. Measured results indicate the feasibility of the method for designing the stiffness of deployable antennas.

Nomenclature

$[E]$	= identity matrix
EJ	= flexural rigidity, N · mm^2
f_i	= system natural frequencies, Hz
I	= moment of inertia about hinge line, N · mm · s^2
$[K]$	= stiffness matrix
K_{θ_j}	= rotational spring constant of the antenna deployment mechanism, N/mm
L	= beam length, mm
$[M]$	= mass matrix
m	= number of nodes
n	= number of elastic modes
$\{q\}$	= generalized coordinates
q_i	= generalized coordinates of elastic modes
$[R]$	= matrix defined by $[R_1 \;\; R_2 \;\; R_3]$
$\{\boldsymbol{R}_1\}, \{\boldsymbol{R}_2\}, \{\boldsymbol{R}_3\}$	= rotational rigid body vectors, rad
T	= kinetic energy
U	= potential energy
$\{u\}$	= displacement in the structural system
$\{u_f\}$	= elastic displacement of reflector
$\{u_r\}$	= rigid-body displacement of reflector due to rotation
X_p, Y_p, Z_p	= coordinates of node p, mm
$\{\boldsymbol{\theta}\}$	= rotation angle vector defined by $\{\theta_1, \theta_2, \theta_3\}^T$, rad
$\theta_1, \theta_2, \theta_3$	= rotation angles about X, Y, and Z axes, rad
ρ	= mass per length, kg · s^2/mm^2
$[\phi]$	= modal matrix defined by $[\phi_1 \;\; \phi_2 \;\; \cdots \;\; \phi_n]$
$\{\phi_i\}$	= ith normal mode of reflector
Ω_i	= system angular frequency, Hz
ω_i	= angular frequency of reflector, Hz
ω_{θ_j}	= angular frequency corresponding to the rigid-body rotation of reflector, Hz

Subscripts

i	= mode number
j	= rotational coordinates ($1 \equiv X$, $2 \equiv Y$, and $3 \equiv Z$)

Introduction

STIFFNESS is one of the important design requirements placed on satellite antennas in their deployed configurations. Vibration caused by thruster activity degrades the performance of both the attitude control system and the antenna pointing control system. Therefore, satellite antennas have to meet specified frequency requirements to avoid coupling with these control systems. The size of satellite antennas will, however, increase to upgrade communication capability. Deployable antennas are currently being studied as one candidate in developing large-satellite antennas because they overcome the shroud limitation of launch vehicles. Inasmuch as natural frequencies decrease with increasing antenna diameter, stiffness will become more important for large antennas.

In many deployable antennas,[1–6] natural frequencies of the deployed antenna vary with the antenna deployment mechanism (ADM). Early ADM designs, however, did not consider stiffness in determining the dynamic behavior of the antenna.[7] Therefore, it was unclear how the ADM affected the antenna's vibration characteristics. The lack of ADM data also complicated stiffness designs. The increased size and flexibility of satellite antennas after deployment limit the validity of data acquired on the ground by vibration tests.[8] Thus, an analytical approach is the only way of validating the stiffness design of large antennas.

In stiffness design of large deployable antennas, we are first faced with the difficult problem of how to predict frequencies in orbit. Finite element method (FEM) analysis can give no meaningful frequency information without the stiffness data of the ADM. Therefore, we cannot use FEM analysis for frequency prediction. FEM analysis can be used only to confirm natural frequencies after the stiffness data of the ADM are measured. Yet even in the early design stage, the frequency requirement of the deployable antennas must be satisfied. A new design method that ensures the stiffness of large deployable antennas is, therefore, needed.

An efficient method, which establishes the stiffness requirement for the ADM, is proposed for large deployable antennas. This method establishes the interface condition between the ADM and the reflector and, thus, ensures that the deployable antenna meets the frequency requirement. This method also makes it possible to

Received May 14, 1997; revision received Nov. 17, 1997; accepted for publication Nov. 22, 1997. Copyright © 1998 by the American Institute of Aeronautics and Astronautics, Inc. All rights reserved.

*Senior Research Engineer, Wireless Systems Laboratories, Spacecraft Structure Group, Yokosuka-shi. Senior Member AIAA.

†Professor, Department of Mechano-Aerospace Engineering, Meguro-ku. Member AIAA.

confirm, at all design phases, whether the antenna satisfies the frequency requirements. The deployable antenna is first modeled as an elasticity body supported by a coil spring, and a theoretical formulation of the system is described. Next, we describe the effects of ADM stiffness on the first frequency of the antenna and then show the procedure to establish the stiffness requirement for the ADM. Next, the design method is applied to an antenna on the Japanese Engineering Test Satellite VI (ETS-VI) launched in 1994. The effectiveness of this method is proved by comparing predicted frequencies with frequencies measured in orbit.

Frequency Analysis

Finite Element Model of Reflector

Consider a deployable antenna consisting of a reflector supported by an ADM. Figure 1 shows the analytical model of the deployable antenna. The Cartesian coordinate system shown in Fig. 1 is used in this study. Note that the X axis points along the hinge. The reflector is an elastic body, and its vibration characteristics with ADM interface fixed are considered in the formulation. The ADM is modeled as a coil spring, and its mass is neglected because its first natural frequency is high. The displacement of the antenna can be expressed as the sum of the elastic displacement $\{u_f\}$ and rigid-body displacement $\{u_r\}$ due to spring rotation. Therefore, we obtain the following relation:

$$\{u\} = \{u_f\} + \{u_r\} \tag{1}$$

The elastic displacement $\{u_f\}$ satisfies the undamped equation of motion for the reflector, expressed as

$$[M]\{\ddot{u}_f\} + [K]\{u_f\} = \{0\} \tag{2}$$

Therefore, we can rewrite the elastic displacement using normal modes $[\phi]$ as

$$\{u_f\} = [\phi]\{q\} \tag{3}$$

On the other hand, the rigid-body displacement $\{u_r\}$ due to rotation of the reflector is given by

$$\{u_r\} = [R]\{\theta\} \tag{4}$$

Matrix $[R]$ consists of the unit rotation vector about the X, Y, and Z axes. Each unit rotation vector is defined by

$$\begin{aligned}\{\boldsymbol{R}_1\} &= \{0, -Z_1, Y_1, 1, 0, 0, \ldots, 0, -Z_m, Y_m, 1, 0, 0\}^T \\ \{\boldsymbol{R}_2\} &= \{Z_1, 0, -X_1, 0, 1, 0, \ldots, Z_m, 0, -X_m, 0, 1, 0\}^T \\ \{\boldsymbol{R}_3\} &= \{-Y_1, X_1, 0, 0, 0, 1, \ldots, -Y_m, X_m, 0, 0, 0, 1\}^T\end{aligned} \tag{5}$$

The displacements of the reflector are expressed in the form

$$\{u\} = \sum_{i=1}^{n} q_i\{\phi_i\} + \sum_{j=1}^{3} \theta_j\{\boldsymbol{R}_j\} \tag{6}$$

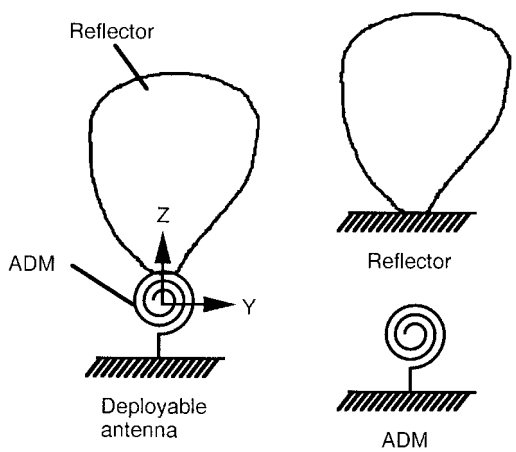

Fig. 1 Analytical model of deployable antenna.

For $\{\boldsymbol{R}\}$ and θ, we use the notation $1 \equiv X$, $2 \equiv Y$, and $3 \equiv Z$. Using this displacement, the kinetic energy of the system is given by

$$2T = \{\dot{u}\}^T[M]\{\dot{u}\} \tag{7}$$

Substitution of Eq. (6) into Eq. (7) leads to the following equation:

$$\begin{aligned}2T = &\sum_{i=1}^{n} \dot{q}_i^2\{\phi_i\}^T[M]\{\phi_i\} + 2\sum_{i=1}^{n}\sum_{j=1}^{3} \dot{q}_i\dot{\theta}_j\{\boldsymbol{R}_j\}^T[M]\{\phi_i\} \\ &+ \sum_{i=1}^{3}\sum_{j=1}^{3} \dot{\theta}_i\dot{\theta}_j\{\boldsymbol{R}_i\}^T[M]\{\boldsymbol{R}_j\}\end{aligned} \tag{8}$$

Next, the potential energy of the system is given by

$$\begin{aligned}2U &= \sum_{i=1}^{n}\{\phi_i\}^T[K]\{\phi_i\} + \sum_{j=1}^{3} K_{\theta_j}\theta_j^2 \\ &= \sum_{i=1}^{n} \omega_i^2 q_i^2\{\phi_i\}^T[M]\{\phi_i\} + \sum_{j=1}^{3} K_{\theta_j}\theta_j^2\end{aligned} \tag{9}$$

The system equation of motion, obtained by substituting Eqs. (8) and (9) into Lagrange's equation, can be expressed as

$$[A]\{\ddot{\boldsymbol{\xi}}\} + [B]\{\boldsymbol{\xi}\} = \{0\} \tag{10}$$

where

$$\{\boldsymbol{\xi}\} = \{q_1 \quad q_2 \quad \cdots \quad q_n \quad \theta_1 \quad \theta_2 \quad \theta_3\}^T \tag{11}$$

$$[A] = \begin{bmatrix} P_{11} & 0 & P_{1,n+1} & P_{1,n+2} & P_{1,n+3} \\ & P_{22} & P_{2,n+1} & P_{2,n+2} & P_{2,n+3} \\ & & \ddots & \vdots & \vdots & \vdots \\ & & P_{nn} & P_{n,n+1} & P_{n,n+2} & P_{n,n+3} \\ & & & P_{n+1,n+1} & P_{n+1,n+2} & P_{n+1,n+3} \\ & \text{symmetry} & & & P_{n+2,n+2} & P_{n+2,n+3} \\ & & & & & P_{n+3,n+3} \end{bmatrix} \tag{12}$$

$$[B] = \begin{bmatrix} P_{11}\omega_1^2 & & & & \\ & P_{22}\omega_2^2 & & 0 & \\ & & \ddots & & \\ & & & P_{nn}\omega_n^2 & \\ & & & & P_{n+1,n+1}\omega_{\theta_1}^2 \\ & 0 & & & P_{n+2,n+2}\omega_{\theta_2}^2 \\ & & & & & P_{n+3,n+3}\omega_{\theta_3}^2 \end{bmatrix} \tag{13}$$

It is readily seen from Eq. (13) that there is no stiffness coupling between the elastic vibration and the rigid-body rotation. The parameters P are defined by

$$\begin{aligned}&P_{ii} = \{\phi_i\}^T[M]\{\phi_i\}, \qquad P_{i,n+j} = \{\boldsymbol{R}_j\}^T[M]\{\phi_i\} \\ &P_{n+j,n+j} = \{\boldsymbol{R}_j\}^T[M]\{\boldsymbol{R}_j\} \qquad (i = 1, 2, \ldots, n,\ j = 1, 2, 3)\end{aligned} \tag{14}$$

Here, P_{ii} and $P_{i,n+j}$ are, respectively, the modal mass and the modal momentum of ith mode. $P_{n+j,n+j}$ are the moments of inertia (MOI) about each coordinate axis. The angular natural frequencies ω_{θ_j} are defined by

$$\omega_{\theta_j} = \sqrt{K_{\theta_j}/I} \qquad (j = 1, 2, 3) \tag{15}$$

These represent the rigid-body system angular frequencies of the reflector.

Cantilever Beam Model of Reflector

Many deployed antennas behave as cantilever beams, and so we focus on a cantilever beam model in this section. The cantilever beam model is useful because we require neither FEM analysis nor any consideration of geometry or material properties to obtain the relationship between Ω_1/ω_1 and $\omega_{\theta_1}/\omega_1$.

Given the flexural rigidity constant, the angular natural frequencies of the cantilever beam are given by

$$\omega_i = (\alpha_i/L)^2\sqrt{EJ/\rho} \qquad (i = 1, 2, \ldots, n) \tag{16}$$

where α_i are the roots of the following equation:

$$1 + \cosh\alpha_i \cos\alpha_i = 0 \tag{17}$$

The normal modes at the natural frequencies are

$$\phi_i = (\cos\alpha_i + \cosh\alpha_i)(\cos\alpha_i X/L - \cosh\alpha_i X/L) - (\sin\alpha_i + \sinh\alpha_i)(\sin\alpha_i X/L - \sinh\alpha_i X/L) \tag{18}$$

The parameters P of the cantilever beam are expressed as

$$P_{ii} = \int_0^L \rho\phi_i^2\,\mathrm{d}X, \qquad P_{i,n+1} = \int_0^L \rho X\phi_i\,\mathrm{d}X$$
$$P_{n+1,n+1} = \int_0^L \rho X^2\,\mathrm{d}X \qquad (i = 1, 2, \ldots, n) \tag{19}$$

The ADM has translational stiffness and bending stiffness in three directions. However, only the bending stiffness about the hinge line was considered in the analysis because in most cases only the lower modes of the reflector are bending. This means that the effect of the bending modes dominates the lower frequencies of deployable antennas. Calculating the parameters P from Eqs. (18) and (19), it can be understood that P_{ii}, $P_{i,n+1}$, and $P_{n+1,n+1}$ are in proportion to ρL, ρL^2, and ρL^3. We introduce generalized coordinates for the rotation angles and rewrite the vector using $\{\boldsymbol{R}'_j\}$ as

$$b_i = L\theta_i \tag{20}$$

$$\{\boldsymbol{R}'_j\} = \{\boldsymbol{R}_j\}/L \tag{21}$$

Equation (10) is rewritten using the generalized coordinates

$$\{\eta\} = \{q_1 \quad q_2 \quad \cdots \quad q_n \quad b_1\}^T \tag{22}$$

Then, by dividing both sides by $\rho L\omega_1^2$, the following equation can be obtained:

$$\left(-\Omega^2/\omega_1^2[A'] + [B']\right)\{\eta\} = \{0\} \tag{23}$$

where

$$[A'] = \begin{bmatrix} P'_{11} & 0 & & P'_{1,n+1} \\ & P'_{22} & & P'_{2,n+1} \\ & & \ddots & \vdots \\ \text{symmetry} & & P'_{nn} & P'_{n,n+1} \\ & & & P'_{n+1,n+1} \end{bmatrix} \tag{24}$$

$$[B'] = \begin{bmatrix} P'_{11} & & & 0 \\ & P'_{22}\omega_2^2/\omega_1^2 & & \\ & & \ddots & \\ 0 & & P'_{nn}\omega_n^2/\omega_1^2 & \\ & & & P'_{n+1,n+1}\omega_{\theta_1}^2/\omega_1^2 \end{bmatrix} \tag{25}$$

Note that all of the parameters P', obtained by dividing P by ρL, are constant. The natural frequency ratios of the cantilever beam in Eq. (25), obtained from Eq. (16), are also constant. Thus, the system natural frequencies are independent of both the length and the material characteristics of the cantilever beam. Only the normal modes $\{\phi_i\}$ and the frequency ratios α_i/α_1 are required to obtain the relationship. By normalizing $\{\boldsymbol{R}\}$ and θ using Eqs. (20) and (21), only the frequency ratio $\omega_{\theta_1}/\omega_1$ in Eq. (25) is an unknown. We can obtain the relationship between Ω_1/ω_1 and $\omega_{\theta_1}/\omega_1$ by calculating the frequency ratio Ω_1/ω_1 for given values of $\omega_{\theta_1}/\omega_1$.

Procedure to Establish Stiffness Requirement

Most current reports concerning the ADM deal with function design. There are few stiffness data on the ADM because vibration characteristics have not been considered in ADM design. The FEM is a powerful tool for analyzing many complex structures. However, FEM analysis can give no meaningful frequencies without the ADM stiffness data. This means that we cannot use FEM analysis for frequency prediction. FEM analysis is useful to confirm natural frequencies only after stiffness data for the ADM have been measured. In the following section, we describe a procedure for establishing the stiffness requirement of the ADM so that the frequency requirement of the deployable antenna can be satisfied.

Relationship Between Ω_1/ω_1 and $\omega_{\theta_1}/\omega_1$

Table 1 lists the values of these parameters calculated on the assumption that the mass per unit length is constant for the beam model. The lower three modes were used in the calculation. As described earlier, all parameters are proportional to ρL. Therefore, the system natural frequencies do not depend on any material properties of the beam. Figure 2 shows the variation of the frequency ratio Ω_1/ω_1 with $\omega_{\theta_1}/\omega_1$ using the lower three modes for the beam model. For values of $\omega_{\theta_1}/\omega_1 \leq 1$, the ADM stiffness affects the first natural frequency of the system. The relationship between Ω_1/ω_1 and $\omega_{\theta_1}/\omega_1$ is linear for small $\omega_{\theta_1}/\omega_1$. At $\omega_{\theta_1}/\omega_1 = 1.0$, the first natural frequency of the system decreases by 50% compared to the cantilever beam. As the ratio of $\omega_{\theta_1}/\omega_1$ increases, the frequency Ω_1 asymptotically approaches the first natural frequency of the cantilever beam ω_1. These results show that it is very important to consider the bending stiffness of the ADM when designing the stiffness of deployable antennas.

For the FEM model, the natural frequencies and their modes are obtained by solving Eq. (2). Once the frequency ratios ω_i/ω_1 and the parameters P are calculated, the relationship between Ω_1/ω_1 and $\omega_{\theta_1}/\omega_1$ can be obtained in the same way as the beam model.

Effect of Higher Modes on the First Frequency Ω_1

For simplicity, we consider only the first mode of the cantilever beam or of the reflector. The equation of motion is given by

$$\left(-\frac{\Omega_1^2}{\omega_1^2}\begin{bmatrix} P'_{11} & P'_{12} \\ P'_{12} & P'_{22} \end{bmatrix} + \begin{bmatrix} P'_{11} & 0 \\ 0 & P'_{22}\omega_{\theta_1}^2/\omega_1^2 \end{bmatrix}\right)\{\eta\} = \{0\} \tag{26}$$

Table 1 Parameters P of the cantilever beam

Mode no. i	P_{ii}	P_{i4}	P_{44}
1	ρL	$3.2 \times 10^{-1}\rho L$	$\rho L/3$
2	ρL	$3.5 \times 10^{-3}\rho L$	$\rho L/3$
3	ρL	$7.1 \times 10^{-5}\rho L$	$\rho L/3$

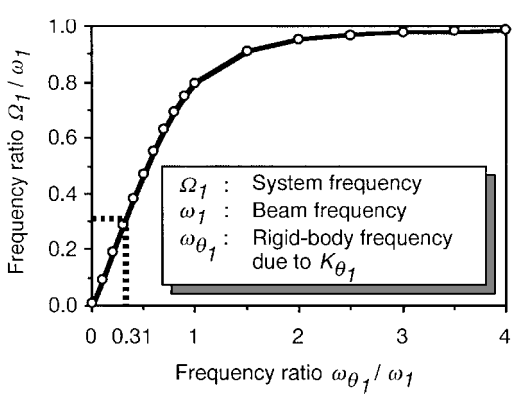

Fig. 2 Variation in the first natural frequency for the cantilever beam.

The characteristic equation is given by

$$\mu\left(\Omega_1^2/\omega_1^2\right)^2 - \left(1+\omega_{\theta_1}^2/\omega_1^2\right)\left(\Omega_1^2/\omega_1^2\right) + \omega_{\theta_1}^2/\omega_1^2 = 0 \qquad (27)$$

where μ is defined as

$$\mu = 1 - P_{12}'^2/P_{11}'P_{22}' \qquad (28)$$

Note that μ satisfies the following condition:

$$0 \le \mu \le 1 \qquad (29)$$

For $\mu \neq 0$, Eq. (27) gives the following solution:

$$\frac{\Omega_1}{\omega_1} = \sqrt{\frac{\left(1+\omega_{\theta_1}^2/\omega_1^2\right) - \sqrt{\left(1+\omega_{\theta_1}^2/\omega_1^2\right)^2 - 4\mu\omega_{\theta_1}^2/\omega_1^2}}{2\mu}} \qquad (30)$$

For $\mu = 0$ we obtain

$$\frac{\Omega_1}{\omega_1} = \sqrt{\frac{\omega_{\theta_1}^2/\omega_1^2}{1+\omega_{\theta_1}^2/\omega_1^2}} \qquad (31)$$

Now, when considering all modes of the cantilever beam, the parameter μ can be derived as

$$\mu_{ij} = 1 - \frac{P_{i,n+j}^2}{P_{ii}P_{n+j,n+j}} \qquad (i=1,2,\ldots,n,\ j=1,2,3) \qquad (32)$$

and we obtain the relationship between Ω_1/ω_1 and $\omega_{\theta_1}/\omega_1$ by solving a characteristic equation of $(n+3)$th degree.

It can be seen from Eq. (30) that the frequency ratio Ω_1/ω_1 depends on the parameter μ. This parameter provides an indication of which modes we must consider from the point of view of prediction accuracy. The effective mass matrix M_{eff} is defined[9] as

$$M_{\text{eff}} = [R]^T[M][\phi][\phi]^T[M][R] \qquad (33)$$

Normalize the mode shapes as

$$[\phi]^T[M][\phi] = [E] \qquad (34)$$

This means P_{ii} is equal to one. If the modal matrix $[\phi]$ includes all mode shapes, we obtain the following relation:

$$[M][\phi][\phi]^T = [E] \qquad (35)$$

Using relation (35), Eq. (33) can be rewritten as

$$M_{\text{eff}} = [R]^T[M][R] \qquad (36)$$

Equation (36) shows that the effective mass matrix M_{eff} is a rigid-mass matrix, considering all mode shapes of the reflector: Diagonal terms are equal to the mass or MOI of the reflector, whereas $P_{i,n+j}^2$ is the effective mass of the ith mode. The sum of $P_{i,n+j}^2$ approaches the mass or MOI as the number of modes approaches the total number of dynamic degrees of freedom. Therefore, $P_{i,n+j}^2/P_{n+j,n+j}$ represents the magnitude of the relative contribution of the ith mode to the overall structural behavior about each coordinate axis. From the point of view of prediction accuracy, we need consider only modes for which the parameter μ has a small value.

The influence of the parameter μ on the frequency ratio Ω_1/ω_1 is shown in Fig. 3 for the beam model. The results were obtained by considering the lower three modes. The curve for $\mu = 1$ shows that no coupling exists between the elastic vibration and the rigid-body rotation. The frequency ratio Ω_1/ω_1 is equal to 1 for values of $\omega_{\theta_1}/\omega_1 > 1$. Therefore, Ω_1/ω_1 is independent of $\omega_{\theta_1}/\omega_1$ in this range. This means that the first frequency of the system is that of the cantilever beam. On the other hand, Ω_1/ω_1 is equal to $\omega_{\theta_1}/\omega_1$ for values of $\omega_{\theta_1}/\omega_1 < 1$. Therefore, the first frequency of the system is determined by the ADM stiffness and the MOI of the beam. These are reasonable results from a physical point of view. As μ becomes small, the frequency ratio Ω_1/ω_1 decreases due to the coupling between the elastic vibration and the rigid-body rotation. The curve for $\mu = 0$ shows the worst-case decrease in the frequency ratio Ω_1/ω_1. For the cantilever beam, the value of μ is 0.7 for the first mode, 1.0 for the second mode, and 1.0 for the third mode. In this case only the first mode affects the natural frequencies of the system.

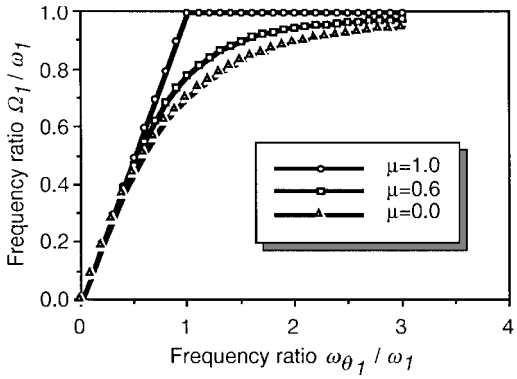

Fig. 3 Influence of parameter μ on the first natural frequency for the cantilever beam.

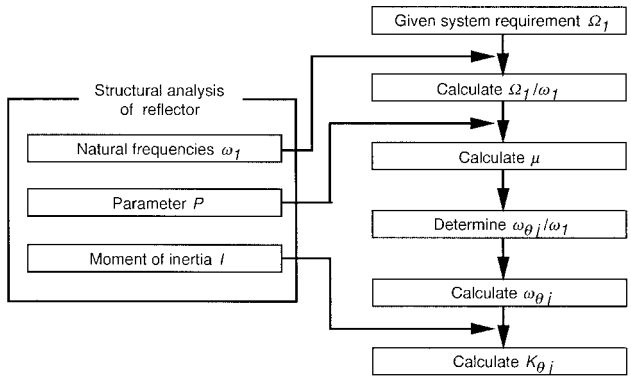

Fig. 4 Flowchart for establishing the stiffness requirement of the ADM.

Procedure

A flowchart diagramming the process of determining the ADM stiffness is shown in Fig. 4. For both the cantilever beam and the reflector, the natural frequencies ω_1, the moment of inertia I, and the parameters P are obtained from a current structural analysis. Next we calculate the parameter μ defined by Eq. (32) and obtain the relationship between Ω_1/ω_1 and $\omega_{\theta_1}/\omega_1$ for the calculated parameter μ. The number of modes considered is determined based on the values of the parameter μ. Given the frequency requirement Ω_1 for the system (deployable antenna), we can obtain the value of Ω_1/ω_1. The value of $\omega_{\theta_1}/\omega_1$ at Ω_1/ω_1 can be found from the appropriate relationship. Finally, the required K_{θ_1} can be derived from Eq. (15). This procedure is very effective for deployable antennas because we can set a value on the stiffness requirement of the ADM so that the deployable antenna satisfies the necessary frequency requirement.

Application to a Deployable Satellite Antenna

Antenna Configuration

As an example, we consider the deployable antenna system on the Japanese ETS-VI. The antenna configuration of the ETS-VI is shown in Fig. 5. The antenna subsystem includes both 20- and 30-GHz-band antennas. The aperture diameters are, respectively, 3.5 and 2.5 m. Each antenna is composed of a reflector, a deployment mechanism (ADM), and hold-down release mechanisms. The antennas are stowed during launch to comply with the shroud diameter limitations of the H-II rocket. They are fixed on an antenna tower and deployed to their in-orbit configurations using the ADM. Antenna deployment is activated by pyrodevices and spring forces. In this paper, the calculated and measured results are described for the 20-GHz-band antenna. The frequency requirement for the 20-GHz-band antenna with satellite interface fixed is more than 1.3 Hz in

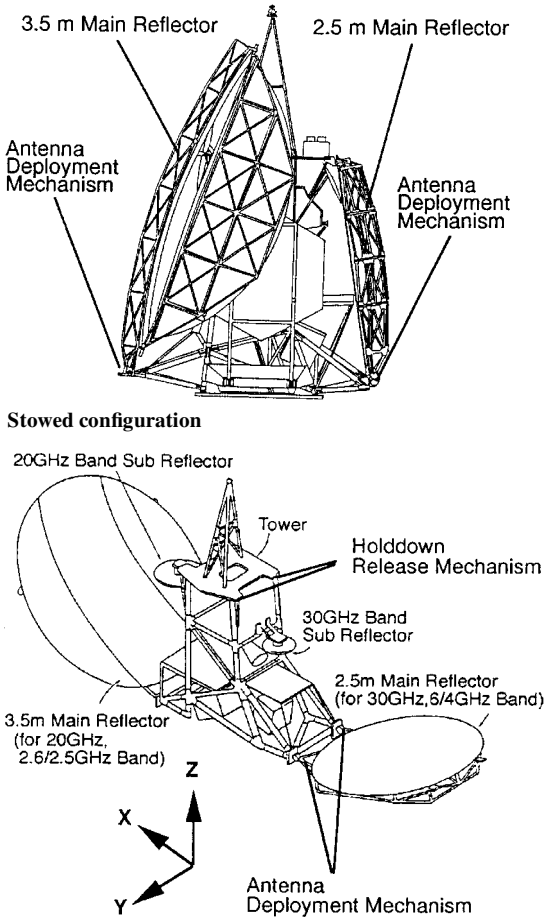

Fig. 5 ETS-VI antenna configuration.

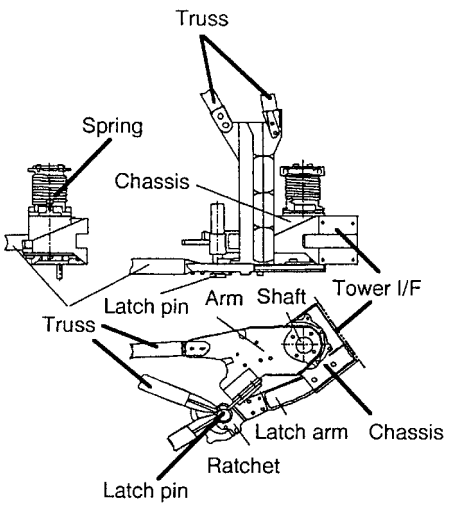

Fig. 6 Detail of ADM.

the deployed configuration. This requirement was established considering coupling with the antenna pointing control.

The ADM consists of two identical hinge mechanisms, each with a ball bearing, a coil spring, an arm, a latch assembly, a shaft, and a chassis. The hinge mechanism is indicated in Fig. 6. The arm is connected to a shaft and interfaces with the reflector. A coil spring provides the driving torque. One end of the spring is fixed to the shaft, and the other end is attached to the chassis. The latch assembly is used to limit deployment movement in the specified position. When deployed, the latch pin comes in contact with the pair of latch arms mounted on the side of the chassis. This pin is fixed by ratchets to prevent back travel.

Table 2 Parameter values for the beam model

Parameter	Value
Beam length L	4.40×10^3 mm
Displacement u	1.42 mm
Flexural rigidity EJ	1.96×10^{11} N · mm^2
Density per length ρ	9.42×10^{-7} kg · s^2/mm^2
Coefficient α_1	1.88
First angular frequency ω_1	26.4 Hz
Moment of inertia I	2.62×10^5 N · mm · s^2
Rigid-body angular frequency ω_θ	9.86 Hz

Table 3 Natural frequencies and respective modes for the 3.5-m reflector

Mode no.	Frequency, Hz	Mode
1	3.83	Z bending
2	8.76	Z bending with torsion
3	21.6	Z bending with torsion

Table 4 Parameter P of the 3.5-m reflector

Mode no. i	P_{ii}	P_{i4}	P_{44}	μ
1	1.00	41.5	2.67×10^4	0.93
2	1.00	0.574	2.67×10^4	1.00
3	1.00	2.95	2.67×10^4	1.00

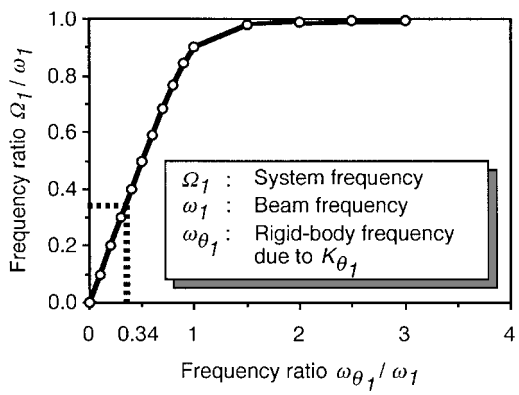

Fig. 7 Variation in the first natural frequency for the 3.5-m antenna.

Analytical Vibration Characteristics of the Reflector

We use two models to establish the stiffness requirements: a beam model and an FEM model. The FEM model has 1400 nodes and 1600 elements. To obtain the beam model, the deflection u_{tip} at the tip of the reflector with 9.8-N force applied along the out-of-plane line was calculated using the FEM model. The boundary condition is that the reflector is fixed at its interface with the ADM. The flexural rigidity EJ can be obtained from

$$EJ = \frac{L^3}{3u_{\text{tip}}} \tag{37}$$

The first natural frequency of the cantilever beam, 4.2 Hz, is obtained from Eq. (16). The data used to calculate ω_1 and ω_{θ_1} are summarized in Table 2. The MOI about the hinge line is the result of FEM analysis. Next, the natural frequencies and their respective modes were calculated using the FEM model. The boundary condition is the same as that for the beam model mentioned earlier. The calculated result is listed in Table 3. The parameters P and μ were also calculated and are shown in Table 4. The first natural frequency of the beam model is a little bit higher than that of the FEM model. The value of the parameter μ for the first mode is different between the FEM and beam models. This difference is caused by the assumption that mass distribution is uniform along the beam axis. The relationship between Ω_1/ω_1 and $\omega_{\theta_1}/\omega_1$ is shown in Fig. 7. Figures 2 and 7 show that the frequency ratio Ω_1/ω_1 for the FEM model is higher than that for the beam model for values of $\omega_{\theta_1}/\omega_1 > 0.6$. In this case, therefore, the beam model is a good representation of the FEM model if the value of $\omega_{\theta_1}/\omega_1$ is greater than 0.6.

ADM Bending Stiffness

We first establish the ADM stiffness requirement using the beam model. The data indicated in Table 2 are used in the following calculation. As the system requirement f_1 for the 20-GHz-band antenna is more than 1.3 Hz ($\Omega_1 \geq 8.2$), we obtain $\Omega_1/\omega_1 \geq 0.31$. From Fig. 2, the value of $\omega_{\theta_1}/\omega_1$ at $\Omega_1/\omega_1 = 0.31$ is found to be 0.31. Therefore, ω_{θ_1} should be more than 8.1. The ADM stiffness requirement in newton millimeter per radian is obtained as

$$K_{\theta_1} \geq I\omega_{\theta_1}^2 = 1.71 \times 10^7 \tag{38}$$

The stiffness requirement can be derived in a similar way from the FEM model. As $\Omega_1 \geq 8.2$ and $\omega_1 \geq 24.1$, we obtain $\Omega_1/\omega_1 \geq 0.34$. From Fig. 7, the value of $\omega_{\theta_1}/\omega_1$ at $\Omega_1/\omega_1 = 0.34$ is found to be 0.34. Therefore, ω_{θ_1} is more than 8.2, and an ADM stiffness requirement of 1.72×10^7 N · mm/rad is obtained. The two models give almost the same stiffness requirement. Though the parameter μ has different values, depending on the model, the frequency ratio Ω_1/ω_1 is independent of μ for small $\omega_{\theta_j}/\omega_1$.

A static load test was performed to confirm the ADM bending stiffness about the hinge line. The ADM was attached to a jig fixed to a stiff test bed. The measured force–displacement relationship is shown in Fig. 8. The translational stiffness, obtained by curve fitting, is 637 N/mm. The bending stiffness K_{θ_1} is related to the translational stiffness K_1 as follows:

$$K_{\theta_1} = K_1 L_r^2 \tag{39}$$

where L_r (200 mm) denotes the length from the tower interface of the ADM to the latch pin. As a result, a bending stiffness of 2.55×10^7 N · mm/rad, which meets the stiffness requirement, is obtained.

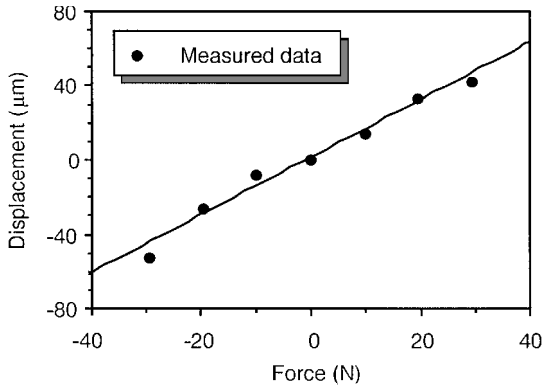

Fig. 8 Measured force–displacement relationship of the ADM.

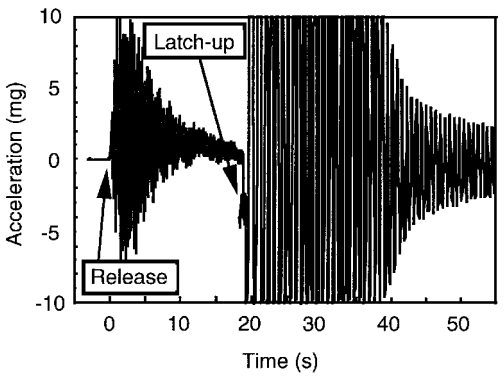

Fig. 9 In-orbit acceleration response of the 3.5-m antenna.

Comparison Between Predicted and Measured Data

The measured stiffness of the ADM enables one to predict the first frequency of the 20-GHz-band antenna. The rigid-body frequency ω_{θ_1}, obtained from Eq. (15), is 9.9 Hz, and the resulting frequency ratio $\omega_{\theta_1}/\omega_1$ is 0.41. From the relationship between Ω_1/ω_1 and $\omega_{\theta_1}/\omega_1$, shown in Fig. 7, the value of Ω_1/ω_1 at $\omega_{\theta_1}/\omega_1 = 0.41$ is 0.40. Therefore, the predicted first frequency of the 20-GHz-band antenna is 1.5 Hz.

The ETS-VI satellite was launched by an H-II rocket in August 1994. Figure 9 shows the acceleration response of the 20-GHz-band antenna in orbit.[10] The antenna was released from the tower at time $t = 0$ s. Acceleration during deployment continued for 20 s. The subsequent acceleration shows free decay after latchup of the antenna. Because the main objective was to measure the acceleration generated by the thruster jet, the maximum range of the accelerometer was set at 10 mg. This explains why the acceleration amplitude exceeded the maximum range immediately after latchup. The first frequency in the deployed configuration was obtained using two methods: One is curve fitting to the free decay data, and the other is

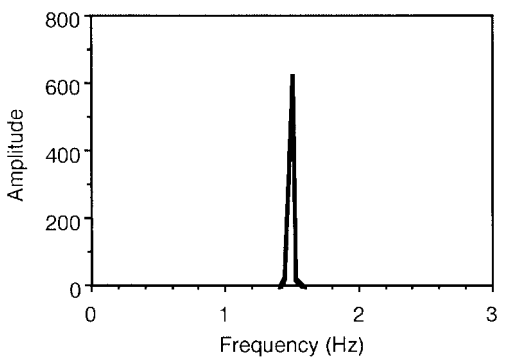

Fig. 11 Results of FFT analysis.

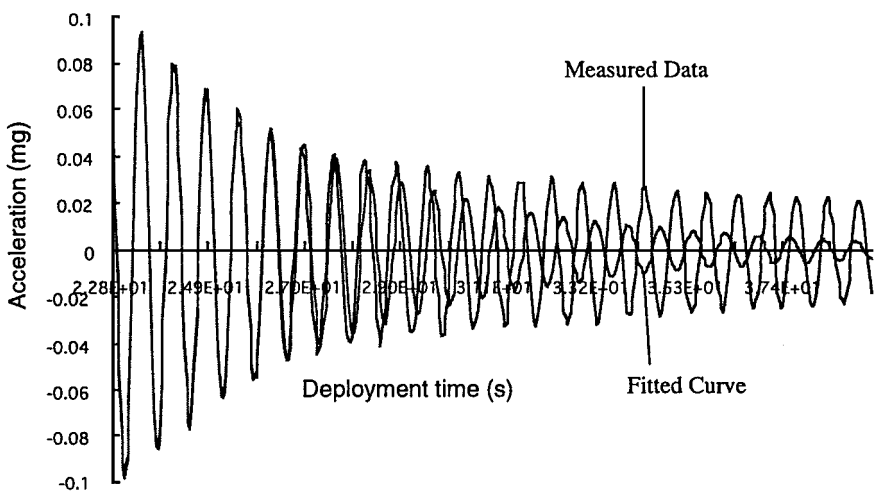

Fig. 10 Results of curve fitting.

fast Fourier transform (FFT) analysis. Figure 10 shows the result of curve fitting. The first frequency may be higher than the identified frequency of 1.42 Hz. It can be seen that there is an error due to curve fitting because only the first mode is considered for frequency identification. Figure 11 shows the result of the FFT analysis. The first frequency is 1.48 Hz. Two results are almost identical and satisfy the frequency requirement.

Conclusion

A design method for meeting the stiffness requirement of deployable satellite antennas in a deployed configuration has been developed. In this method, the deployable antenna is modeled as a structural system in which an elastic body (reflector) is supported by a coil spring (ADM). Displacement of the reflector in the system is expressed as the sum of an elastic displacement and a rigid-body displacement due to spring rotation. The system vibration equation was obtained based on this assumption. Two models were used in this study: a beam model and an FEM model. The beam model is very useful for establishing the stiffness requirements of the ADM because no FEM analysis is required. A procedure to establish the stiffness requirement for the ADM is provided.

By applying the method to a deployable antenna for the Japanese ETS-VI, we established the ADM stiffness requirement. It was also shown by static load tests that the ADM meets the requirement. To confirm the proposed design method, frequencies of the deployable antenna were measured in orbit. Results indicate the feasibility of applying the method to the stiffness design of deployable antennas.

References

[1]Zatychec, W., "ANIK C Space Segment for Telesat Canada," AIAA Paper 80-0474, April 1980.

[2]Misawa, M., Kumazawa, H., and Minomo, M., "Configuration and Performance of 30/20 GHz Band Shaped-Beam Antenna for Satellite Use," AIAA Paper 84-0868, May 1984.

[3]Johnston, W. A., Jr., "ATS-6 Experimental Communications Satellite—Report on Early Orbital Results," *Journal of Spacecraft and Rockets*, Vol. 13, No. 2, 1976, pp. 91–98.

[4]Fager, J. A., "Status of Deployable Geo-Truss Development," *Large Space Antenna System Technology*, NASA CP-2269, May 1982, pp. 513–520.

[5]Mitsugi, J., and Yasaka, T., "A Modular Approach to Build a Large Space Antenna," International Astronautical Federation, IAF-91-315, Oct. 1991.

[6]Misawa, M., "Deployment Reliability Prediction for Large Antenna Driven by Spring Mechanism," *Journal of Spacecraft and Rockets*, Vol. 31, No. 5, 1994, pp. 878–882.

[7]Stella, D., Morgant, F., and Nielsen, G., "Contraves Antenna Tip Hinge Mechanism for Selenia Spazio's 20/30 GHz Antenna," *Proceeding of the 2nd ESA Workshop on Mechanical Technology for Antennas*, European Space Agency, Paris, 1986, pp. 185–194.

[8]Kuo, C. P., and Wada, B. K., "Truss Space Structures System Identification Using the Multiple Boundary Condition Test Method," *AIAA Journal*, Vol. 28, No. 7, 1990, pp. 1246–1249.

[9]Shunmugavel, P., "Modal Effective Masses for Space Vehicles," AIAA Paper 95-1252, May 1995.

[10]Meguro, A., "In-Orbit Deployment Performance of Large Satellite Antennas," *Journal of Spacecraft and Rockets*, Vol. 33, No. 2, 1996, pp. 222–227.

R. B. Malla
Associate Editor